

DEUTSCHES ELEKTRONEN-SYNCHROTRON **DESY**

DESY 76/06
January 1976



Scaling and Impact Parameter Structure in pp Scattering

E. A. Bartnik and J. M. Namysłowski

Institute of Theoretical Physics, Warsaw University

A. M. Din

Institute of Theoretical Physics, Göteborg University

Z. J. Rek

Deutsches Elektronen-Synchrotron DESY, Hamburg

2 HAMBURG 52 · NOTKESTIEG 1

To be sure that your preprints are promptly included in the
HIGH ENERGY PHYSICS INDEX,
send them to the following address (if possible by air mail) :

DESY
Bibliothek
2 Hamburg 52
Notkestieg 1
Germany

Scaling and Impact Parameter Structure in pp Scattering

by

E.A. Bartnik and J.M. Namysłowski
Institute of Theoretical Physics, Warsaw University

A.M. Din
Institute of Theoretical Physics, Göteborg University

Z.J. Rek ⁺⁾
Deutsches Elektronen-Synchrotron DESY, Hamburg

⁺⁾ On leave of absence from Institute of Nuclear Research, Warsaw

Abstract

We attempt to refine and extend the predictions of geometrical scaling by describing deviations from a simple geometric pomeron picture in the P_{lab} region above 20 GeV by the effect of a real, energy-independent, relativistic potential. Our model predictions for σ_{tot} , $\frac{d\sigma}{dt}$ and $\rho = \frac{\text{Re } A}{\text{Im } A} \Big|_{t=0}$

are in fair agreement with existing pp data. The extension of the scheme to $\bar{p}p$ scattering is also presented. We work within an impact parameter framework which renders a convenient symmetric impact parameter state formalism by the use of proper canonical variables. The latter are applied in a phenomenological study of differential cross sections, so as to obtain information about the analytic structure of the scattering amplitude in the impact parameter plane.

I. Introduction

The ever increasing amount of experimental data on pp scattering calls for a flexible phenomenological analysis as well as preferably simple theoretical frameworks. The main points of current interest include the behaviour of total cross sections from intermediate energies up to ISR energies and in the asymptotic region beyond ISR, the detailed structure and energy dependence of the differential cross section and the energy dependence of the scattering amplitude phase.

For $\bar{p}p$ scattering experiments do not extend so far up in energy and consequently the analysis of the transition between the asymptotic region, where pp and $\bar{p}p$ scattering are expected to show similar features, and intermediate energies is not so clear. Also at lower energies, say below $p_{\text{lab}} \sim 50$ GeV spin effects in pp scattering should be appreciable and more complicated models involving the different helicity amplitudes have to be constructed to fit the available polarization data ¹⁾. In the following it will be assumed that corrections due to spin effects can be neglected. The concept of geometrical scaling (GS) ²⁾ has been successful in describing some gross features of $\frac{d\sigma}{dt}$ for pp scattering ^{*)}

*) It should be noted that the forward diffraction peak, down to the minimum, can be described by a universal energy-independent and also process-independent curve even at very low energies if the quantity $\frac{d\sigma}{dt} \left(\frac{d\sigma}{dt} \Big|_{t=0} \right)^{-1}$ is plotted versus $-t \frac{d\sigma}{dt} \Big|_{t=0} \sigma_{\text{el}}^{-1}$, as shown by V. Singh and S.M. Roy, Phys. Rev. Lett. 24(1970)28 and Phys. Rev. D1(1970)2638. This feature extends also up to ISR energies, according to private communication by Professor V. Singh.

such as the energy variation of the dip and second maximum position. With further assumptions one may also see a connection with KNO scaling ³⁾. Although the range of validity of GS has been studied extensively ⁴⁾ its theoretical basis is not quite clear. If cross sections behave asymptotically like $\ln^2 s$ there exist rigorous results ⁵⁾ actually proving GS. At present it is hard to distinguish between a $\ln s$ or a $\ln^2 s$ behaviour experimentally, although our fits to the data seem

to favour slightly the latter possibility.

Being a geometric concept GS is naturally formulated in an impact parameter space (using however a mixed representation). Physically we interpret GS as the effect of a geometric pomeron which dominates the scattering at asymptotic energies and thus characterizes the rising cross sections. The effect of the geometric pomeron may be extrapolated downwards in energy (as exemplified by the smooth σ_{in} for pp scattering) but at lower energies it will be changed by other effects giving rise to the detailed structure of σ_{tot} and $\frac{d\sigma}{dt}$. In a Regge approach these corrections would be determined by the contribution of the different Regge trajectories. In spite of the popularity and good agreement with experiment of Regge models they have two important drawbacks: a large number of unknown parameters and a rather unnatural position of the pomeron among the other Regge trajectories.

We will attempt to describe the corrections to GS by a relativistic, energy-independent potential ⁶⁾. This may of course be thought of as connected with the ρ -meson Regge trajectory exchange. However in this language we find that apart from the Regge pole term there must be at least one Regge cut which actually gives a stronger contribution than the ρ -Regge pole.

Essential to the impact parameter approach ⁷⁾ is the use of canonical variables ^{6,8)}, so as to be in accordance with general principles of quantum mechanics, leading to a more physical phenomenological analysis. We choose impact parameters which make the scattering formalism symmetric with respect to incoming and outgoing impact parameter states and display explicitly the time reversal invariance of the amplitude.

The plan of the paper is as follows: In section II we define the impact parameter approach in terms of our canonical variables and construct the scattering theory. Some further details are given in an appendix. The relativistic, energy-independent potential is introduced in section III and the expression for the scattering amplitude is derived in the eiko-

nal approximation. This contribution is added to the GS part and the requirements of crossing symmetry are discussed. In section IV we give the parametrization of the GS and potential parts as fitted to some appropriately chosen σ and $\frac{d\sigma}{dt}$ data. Subsequently the model predictions for σ_{tot} , $\frac{d\sigma}{dt}$ and $\rho = \frac{\text{Re } A}{\text{Im } A} \Big|_{t=0}$ are compared to the experimental pp data. The more experimentally inclined reader may jump directly to this section. The corresponding extension of the model to $\bar{p}p$ scattering is discussed in section V. A phenomenological analysis of some pp data is performed in section VI using our impact parameter variables. Finally in section VII follows a discussion of our approach and results.

II. The Impact Parameter Formalism

In the classical theory of scattering the concept of an impact parameter is very natural and simple since it is directly related to the geometry of the scattering process but in quantum theory one has to make sure that the scattering variables are chosen as commuting observables. Besides the proper choice of canonical variables there is also the specific quantum mechanical problem of choosing asymptotic scattering states fulfilling certain physical requirements. The impact parameter representation ⁷⁾ has been studied in particular by Chang and Raman, and more recently Elvekjaer and Petersen ⁸⁾ reconsidered the formalism with special emphasis on the use of canonical variables. In this work there was a distinct asymmetry between incoming and outgoing states, which is absent in our approach due to the choice of some new canonical variables.

Let us start by considering elastic scattering of two particles with masses m_1 and m_2 . Although one might go through the formalism in the general case we will for simplicity state our results for the case $m_1 = m_2$ (e.g. pp scattering). Also complications due to spin will be neglected. The incoming momenta are denoted by q_1, q_2 and the outgoing ones by p_1, p_2 . The total 4-momentum is $P = q_1 + q_2 = p_1 + p_2$ and we have the usual invariants $s = P^2 (>0)$, $t = (q_1 - p_1)^2$ and $u = (q_1 - p_2)^2$. In the unequal mass case one may define the so called Wightman-Gårding vectors

$$\begin{aligned}
 q &= \frac{1}{2} (q_1 - q_2) - (m_1^2 - m_2^2) P/2s \\
 p &= \frac{1}{2} (p_1 - p_2) - (m_1^2 - m_2^2) P/2s
 \end{aligned}
 \tag{2.1}$$

which in the equal mass case become simply

$$\begin{aligned}
 q &= \frac{1}{2} (q_1 - q_2) \\
 p &= \frac{1}{2} (p_1 - p_2)
 \end{aligned}
 \tag{2.2}$$

For on-shell scattering $q_1^2 = q_2^2 = p_1^2 = p_2^2 = m^2$ we notice that q and p are perpendicular to P , i.e. $p \cdot P = q \cdot P = 0$. Let us further introduce the average momentum $\kappa = \frac{1}{2} (q + p)$ ($\kappa^2 < 0$) and two other spacelike vectors e_1 and e_2 with $e_1^2 = e_2^2 = -1$ perpendicular to each other as well as to P and κ . We thus have an orthogonal set of 4-vectors (P, κ, e_1, e_2) where P is timelike and κ, e_1, e_2 are spacelike. For an arbitrary 4-vector one may write decomposition $v = v_P \hat{P} + v_{\parallel} \hat{\kappa} + v_{\perp} \hat{e}$ where $\hat{P} = P/\sqrt{P^2}$, $\hat{\kappa} = \kappa/\sqrt{-\kappa^2}$ and \hat{e} is in the (e_1, e_2) plane with $\hat{e}^2 = -1$. The projections $v_P, v_{\parallel}, v_{\perp}$ are relativistic invariants and $v^2 = v_P^2 - v_{\parallel}^2 - v_{\perp}^2$. Making the transition to the c.m. system one sees that the 3-vectors $\vec{q}_1 \rightarrow \vec{q}, \vec{q}_2 \rightarrow -\vec{q}$ and $\vec{p}_1 \rightarrow \vec{p}, \vec{p}_2 \rightarrow -\vec{p}$. Since all relative momentum 4-vectors have a vanishing P -component in this system in effect we have only space-like 3-vectors in the translated (P, κ, e_1, e_2) frame. It is now easy to see that

$$\begin{aligned}
 P_{\parallel} &= q_{\parallel} \\
 P_{\perp} &= -q_{\perp}
 \end{aligned}
 \tag{2.3}$$

and it follows that

$$\begin{aligned}
 s &= 4 (q_{\parallel}^2 + q_{\perp}^2 + m^2) \\
 t &= -4 q_{\perp}^2 \\
 u &= -4 q_{\parallel}^2
 \end{aligned}
 \tag{2.4}$$

We now introduce the two-dimensional impact parameter as the coordinate

space variable canonically conjugate to the transverse momentum, i.e. for the incoming particle we have the pair of variables $(\vec{b}_i, \vec{q}_\perp)$ and for the outgoing one $(\vec{b}_f, \vec{p}_\perp)$. This allows us to have a symmetric impact parameter description of initial and final states in contrast to earlier approaches⁸⁾. As stated above spin will be neglected in constructing the scattering formalism; if it however were to be included the spin quantization axis should presumably be taken along our parallel direction.

In terms of the free two-particle states $|q_\parallel, \vec{q}_\perp\rangle$ in the c.m. system we define the impact parameter states (IPS) as

$$|q_\parallel, \vec{b}\rangle = \frac{1}{2\pi} \int \frac{d^2q_\perp}{2W} e^{-i\vec{b}\cdot\vec{q}_\perp} |q_\parallel, \vec{q}_\perp\rangle \quad (2.5)$$

where $W \equiv q^0 = (q_\parallel^2 + q_\perp^2 + m^2)^{1/2}$. The amplitude for transition between initial IPS $|q_\parallel, \vec{b}_i\rangle$ and final IPS $|p_\parallel, \vec{b}_f\rangle$ is derived in the appendix with the result of equation (A.7):

$$T(q_\parallel, \vec{b}) = \int \frac{d^2q_\perp}{(2\pi)^2} e^{-i\vec{q}_\perp\cdot\vec{b}} \frac{F(q_\parallel, \vec{q}_\perp)}{4q\sqrt{s}} \quad (2.6)$$

where $\vec{b} = \vec{b}_i + \vec{b}_f$, $q = (q_\parallel^2 + q_\perp^2)^{1/2}$ and s is given by (2.4) and $F(q_\parallel, \vec{q}_\perp)$ is the invariant Feynman amplitude. The inverse relation is

$$F(q_\parallel, \vec{q}_\perp) = 4q\sqrt{s} \int d^2b e^{i\vec{q}_\perp\cdot\vec{b}} T(q_\parallel, \vec{b}) \quad (2.7)$$

The interesting thing to observe in these transforms is that the transverse momentum is directly related to t by (2.4), i.e. $q_\perp^2 = -\frac{1}{4}t$. Another good feature of (2.6) is that the integration is wholly within the physical region.

It should be emphasized here that the two pairs of variables q_\parallel, q_\perp and s, t , although formally different, are numerically almost indistinguishable in high energy ($p_{lab} > 20$ GeV) small momentum transfers ($|t| < 5$ GeV²)

region considered in the next three sections. The important differences appear only for small energies and large angles and to investigate them we perform a phenomenological analysis of the data from the latter region in section VI.

III. Deviation from Geometrical Scaling

Geometrical scaling may be formulated in different ways ^{2,4,9)}, however we will take the point of view that GS is reflected most clearly in the properties of the inelastic overlap function as indicated by the smoothness of the total inelastic pp cross section down to $p_{lab} \sim 20$ GeV.

The hypothesis of GS amounts to assuming a representation of the form

$$T(q_{\parallel}, \vec{b}) = T^{(0)}(\vec{b}/R(q_{\parallel})) + T^{(1)}(q_{\parallel}, \vec{b}) \quad (3.1)$$

with $T^{(1)}(q_{\parallel}, \vec{b}) \rightarrow 0$ as $q_{\parallel} \rightarrow \infty$. Here we follow section II and use formally variable q_{\parallel} instead of the non-canonical s . Using (2.7) this may be translated into a property of the differential cross section

$$\frac{d\sigma}{dt} = \frac{1}{64\pi} |A|^2 \quad (3.2)$$

where

$$A = (q\sqrt{s})^{-1} F(q_{\parallel}, \vec{q}_{\perp}) \quad (3.3)$$

The universal function R is to be found from experiment and is intuitively interpreted as a measure of the hadron radius as seen from the relation $R \sim \sqrt{\sigma_{tot}}$ valid at large energies.

As there is not sufficient experimental data to determine R , we will consider two possibilities for large s , namely $R^2 \sim \ln s$ and $R^2 \sim \ln^2 s$. The latter possibility represents a saturation of the Froissart bound up

to a constant and is of a particular interest since one can give in this case a rigorous proof of (3.1) based on analyticity arguments ⁵⁾.

In the case of exact GS we define the profile function Γ by

$$A(q_{\parallel}, \vec{q}_{\perp}) = 4i \int d^2b \exp(i\vec{b} \cdot \vec{q}_{\perp}) \Gamma(q_{\parallel}, \vec{b}) \quad (3.4)$$

and the eikonal χ by

$$\Gamma(q_{\parallel}, b) = 1 - \exp(i \chi(q_{\parallel}, b)) \quad (3.5)$$

We thus have

$$\chi_{GS}(q_{\parallel}, b) = \chi_{GS}(b/R(q_{\parallel})) \quad (3.6)$$

The total inelastic cross section is given by

$$\sigma_{in} = \int d^2b [1 - \exp(-2 \text{Im} \chi_{GS})] \quad (3.7)$$

It follows that $\sigma_{in} \sim R^2(q_{\parallel})$ and the fact that the experimental σ_{in} is smooth down to quite small values of $p_{lab} \sim 5$ GeV makes us believe that GS alone gives a realistic description of σ_{in} .

Later in section IV we shall assume that χ_{GS} is purely imaginary (before invoking crossing symmetry). The important point is however that whatever mechanism induces deviations from GS it should not contribute to $\text{Im} \chi$ in the considered energy region.

With this in mind we propose to represent the deviations from GS by the simple ansatz of a real, energy-independent, relativistic potential V . In the energy region we are working it will be sufficient to derive the contribution of the potential to the amplitude in the eikonal approximation. As will be seen in section IV the specific energy dependence thus introduced, which obviously breaks GS, will be able to represent the expe-

rimental data quite well.

In order to find the amplitude for the potential interaction we may for instance start by rewriting the Weinberg infinite momentum propagator ¹⁰⁾ as follows ^{*)}

$$\begin{aligned} G_0 d\eta d^2q_{\perp} &= \{2\eta (1 - \eta) (s - (q_{\perp}^2 + m^2) \eta^{-1} (1 - \eta^{-1}))\}^{-1} d\eta d^2q_{\perp} \\ &= \frac{1}{2} s^{-1/2} (q^2|_{q \cdot P=0} + \frac{1}{4} s - m^2)^{-1} dq_{\parallel} d^2q_{\perp} \quad (3.8) \\ &= \frac{1}{2} m^{-1} (4mE + m^2)^{-1/2} (q^2|_{q \cdot P=0} m^{-1} + E)^{-1} dq_{\parallel} d^2q_{\perp} \end{aligned}$$

where $E = 1/4 sm^{-1} - m$, η is a normalized light cone variable $\eta = 1/2 + (q_0 + q_P) (P_0 + P^r)^{-1}$ with P_0 denoting the time component and P^r the length of the space part of the total momentum P . The position of the pole in eq. (3.8) is at $E = 1/4 sm^{-1} - m$. E has the following properties: i) it vanishes at threshold, ii) in terms of the relative three-momentum in the c.m. system it is $E = 1/2 |\vec{k}|^2 (\frac{1}{2} m)^{-1}$, thus for small \vec{k} , E is simply the known relative kinetic energy corresponding to the reduced mass $1/2 m$, and iii) for an arbitrary momentum E is given in terms of an invariant, so it can be named the relativistic, relative energy. Similarly we call $q^2|_{q \cdot P=0} m^{-1}$ the relative kinetic energy operator. The factor $s^{-1/2} = (4mE + m^2)^{-1/2}$ appearing in front in eq. (3.8) we do not include in the definition of E since it originates from a Jacobian and has no relevance to the position of the pole. Therefore $s^{-1/2}$ is also absent in the definition of the kinetic energy operator $q^2|_{q \cdot P=0} m^{-1}$.

The next step in our reasoning is to write down an eigenvalue equation with E being the eigenvalue. This equation ^{**)} is

^{*)} For the derivation of amplitude in the potential eikonal model based on Weinberg propagator and infinite momentum variables see ref. /11/. Here we only give arguments for the potential independency of energy.

^{**)} Independently of our arguments there are two other supports for this equation. i) The relativistic quantum mechanical approach, given by F. Co-

$$(-q^2|_{q \cdot P=0} m^{-1} + V) \psi = E \psi \quad (3.9)$$

providing V is E -independent. We emphasize that eq. (3.9) is an eigenvalue equation if, and only if E appears only on the right hand side, and in a linear way. Therefore V must be energy-independent. From eq. (3.9) one finds the eikonal approximation to χ choosing as the eikonal direction $\kappa = \frac{1}{2} (q + p)$ (with $\kappa^2 = \frac{1}{4} u$) as follows ¹¹⁾

$$\chi_{\text{pot}} = -m (-u)^{-1/2} \int_{-\infty}^{\infty} V(b^2 + r_{\parallel}^2) dr_{\parallel} \quad (3.10)$$

The corresponding profile (properly normalized) turns out to be

$$\Gamma_{\text{pot}} = \frac{(-u)^{1/2}}{(s - 4m^2)^{1/2}} (1 - e^{i\chi_{\text{pot}}}) .$$

However in practical calculations the

factor in front is almost unity and will be omitted. To get the total profile Γ we simply assume that

$$\Gamma = 1 - \exp(i\chi_{\text{GS}} + i\chi_{\text{pot}}) = \Gamma_{\text{GS}} + \Gamma_{\text{pot}} - \Gamma_{\text{GS}} \Gamma_{\text{pot}} \quad (3.11)$$

Since $\text{Im } \chi_{\text{pot}} = 0$ the relation (3.7) is obviously unaffected.

ester, S.C. Pieper and F.J.D. Serduke, Phys. Rev. C11(1975)1, leads to an integral equation version of this equation after using the result of T. Kato, Pac. J. Math. 15(1965)171. ii) The limiting case of one of the masses becoming infinite gives the proper relativistic Balmer formula for the hydrogen atom. For details see E. Brezin, C. Itzykson and J. Zinn-Justin, Phys. Rev. D1(1970)2349, and I.T. Todorov, Phys. Rev. D3(1971)2351. Our equation should be contrasted with commonly used equation proposed by R. Blankenbecler and R. Sugar, Phys. Rev. 142(1966)1051.

The expression (3.11) is our ansatz for describing scattering in the energy region $p_{lab} > 20$ GeV and one notes that the approach to GS is completely determined by the damping factor $(-u)^{-1/2}$ in equation (3.10).

Before we can apply this it is however necessary to consider the requirements of crossing symmetry^{5,9)}. We will assume the GS part to be even under crossing, i.e. we require $T(v e^{i\pi}, t) = T^*(v, t)$ where $v = \frac{s-u}{2}$. The proper crossing variable is thus $v e^{-i\pi/2}$. In the energy region under consideration we have $v \sim s \sim -u$ so in the GS part we simply have to make the substitution $s \rightarrow s e^{-i\pi/2}$ i.e. $\ln s \rightarrow \ln s - \frac{i\pi}{2}$. In the potential term the damping factor should be written properly as $|u|^{-1/2}$ which makes it invariant under crossing (in the high s limit under consideration), however because of the factor i in the exponent the potential changes sign when going to the crossed reaction. The potential term is thus not invariant under crossing. Also one notes that the real part of the amplitude will now receive important contributions from both Γ_{GS} and Γ_{pot} as will be discussed in the next section.

IV. Model Predictions

Our predictions will be for the quantities σ_{tot} , σ_{in} , σ_{el} , $\frac{d\sigma}{dt}$ and $\rho = \frac{\text{Re } A}{\text{Im } A} \Big|_{t=0}$. If we denote the Fourier transform of the profile $\Gamma(q, \vec{b})$ (for shortness we write q instead of q_{\parallel} and use momentum transfer $\Delta = 2q_{\perp}$) by $\tilde{\Gamma}(q, \vec{\Delta})$ our normalization is such that

$$\sigma_{tot} = 2 \text{Re } \tilde{\Gamma}(q, 0) \quad (4.1)$$

and

$$\rho = - \frac{\text{Im } \tilde{\Gamma}(q, 0)}{\text{Re } \tilde{\Gamma}(q, 0)} \quad (4.2)$$

where $q^2 = s/4 - m^2$ in the forward direction. Also

$$\frac{d\sigma}{dt} = \frac{1}{4\pi} |\tilde{\Gamma}(q, \vec{\Delta})|^2 \quad (4.3)$$

The scaling part has the form

$$\tilde{\Gamma}_{GS}(q, \Delta) = C R^2(q) \phi_{GS}(\tau) \quad (4.4)$$

where $\tau = R \Delta$ and $\phi_{GS}(0) = 1$. The function ϕ_{GS} is fitted to the data for $\frac{d\sigma}{dt}$ at $p_{lab} = 1496$ GeV according to a representation as a sum of Gaussians

$$\phi_{GS}(\tau) = \sum_{i=1}^3 A_i e^{-\beta_i \tau^2} \quad (4.5)$$

We find the best fit to be given by

$$A_1 = 0.82683, \quad A_2 = 0.17587, \quad A_3 = -0.00270,$$

$$\beta_1 = 3.47, \quad \beta_2 = 14.57, \quad \beta_3 = 0.4542.$$

According to (3.10) we have for the potential part

$$\chi_{pot} = -\frac{m}{2q} \int_{-b}^{\infty} V(b, r_{||}) dr_{||} \quad \text{and for the potential itself we assume a}$$

Gaussian shape of the form

$$V(b, r_{||}) = V_0 \exp\left[-w_0(b^2 + r_{||}^2)\right] + V_1 \exp\left[-w_1(b^2 + r_{||}^2)\right] \quad (4.6)$$

This enables us to evaluate all integrals explicitly and give the results in a convenient series form. For instance one easily obtains

$$\begin{aligned} \tilde{\Gamma}_{pot}(q, \Delta) = & - \sum_{n+m>0} \left(\frac{-i\sqrt{\pi}m}{2q}\right)^{n+m} \left(\frac{V_0}{\sqrt{w_0}}\right)^n \left(\frac{V_1}{\sqrt{w_1}}\right)^m \\ & \frac{1}{n!} \frac{1}{m!} \frac{\pi}{nw_0 + mw_1} e^{-\frac{\Delta^2}{4(nw_0 + mw_1)}} \end{aligned} \quad (4.7)$$

This is of course an asymptotic expansion in $\frac{1}{q} \sim \frac{1}{\sqrt{s}}$ and in practice it turns out that all terms but the first few may be safely neglected.

The expressions (4.4) and (4.7) may now be inserted in (3.11) to give the total profile. Next, from a fit to the data for $\frac{d\sigma}{dt}$ at $p_{lab} = 21.1$ GeV we determine the potential parameters in (4.6) with the result $V_0 = 0.6238$, $w_0 = 0.02512$, $V_1 = -0.170$, $w_1 = 0.01259$ in GeV units. Qualitatively this represents a strong repulsive core with range ~ 1 fermi and a small attractive tail. For the function $R^2(s)$ appearing in (3.6) we have considered two different parametrizations which give good fits to σ_{in} : linear and quadratic in $\ln s$. Obviously the most straightforward way would be to perform a fit to σ_{in} data based on the relation $\sigma_{in} \sim R^2(s)$. However, due to the big uncertainties in σ_{in} measurements, this quantity turns out to be rather insensitive to the small changes of parameters whereas the same changes produce fairly big deviations in σ_{tot} and ρ . Therefore we were forced to include the latter in our fit. In this way we found two parametrizations:

$$R_I^2(s) \sim 1 + 0.070 \ln s, \quad (4.8a)$$

$$R_{II}^2(s) \sim 1 + 0.0042 \ln^2 s. \quad (4.8b)$$

The first one is almost exactly equal to the Barger fit ¹²⁾, $R^2(s) \sim 1 + 0.068 \ln s$ and after inclusion of latest data of Carroll et al. ¹³⁾ turns out to give clearly worse fit than (4.8b). Thus we took the second possibility as the final solution to be compared with experiment.

In Figs. 1-3 we display our results for pp scattering. In Fig. 1 the data ¹³⁾ for σ_{tot} , σ_{in} and σ_{el} are given together with model predictions for (4.8b) (solid lines) and (for σ_{tot} only) the Barger fit (dashed lines). In each pair of solid and dashed curves for σ_{tot} the lower one corresponds to GS contribution only.

The ratio of real to imaginary pp amplitude in the forward direction is shown in Fig. 2. The agreement is very good including the change of sign.

In Fig. 3a the data for $p_{lab} = 21.1$ GeV and 1496 GeV which were used to define the free parameters of $V(r)$ and $\phi_{GS}(\tau)$ are presented. Clearly

the agreement for large t at smaller energy is unsatisfactory, mainly because of the oversimplified shape of the potential. The dashed curve represents GS contribution in 21.1 GeV case. Also the 1496 GeV data are not so very well represented by the sum of three Gaussian terms, especially in the dip region.

Finally Fig. 3b displays our predictions for $\frac{d\sigma}{dt}$ in the whole energy range above 20 GeV. The agreement is quite good except for the dip which is observed experimentally already at 200 GeV and appears in our model only about 300 GeV. Since this may be caused by subtle interference effects and consequently would depend strongly on the potential, it should not be too difficult to improve on this point.

V. $\bar{p}p$ Scattering

Compared to $\sigma_{in}(pp)$, $\sigma_{in}(\bar{p}p)$ is not quite smooth down to low values of p_{lab} but shows a broad minimum similar to $\sigma_{tot}(pp)$. Therefore our approach to pp scattering does not translate directly to $\bar{p}p$ scattering by making the simple sign change of the potential as suggested by (3.10).

One possible way out is to make a new fit to $\sigma_{in}(\bar{p}p) \sim \bar{R}^2(s)$ with $\bar{R}^2(s) = R^2(s) + C s^{-1/2}$ as suggested by $\bar{p}p$ data. This is a phenomenological way of including an extra contribution from annihilation. With this modification we may use the inverted pp potential to predict all $\bar{p}p$ data. For $C = 1.48$ GeV the comparison with data¹³⁻¹⁶⁾ is shown in Figs. 4-6. Fig. 4 shows σ_{tot} , σ_{in} , and σ_{el} ; Fig. 5 - ρ in the forward direction and Fig. 6 - $\frac{d\sigma}{dt}$ for $p_{lab} = 50, 100$ and 200 GeV. Except for ρ where the experimental data are also quite ambiguous, the agreement is surprisingly good when one takes into account that apart from one extra parameter all the results are predicted from pp scattering.

There exists another possibility that the $\bar{p}p$ annihilation is described by adding an absorptive part to the pp potential preserving the old $R^2(s)$ from pp scattering. The relations between these two approaches will be discussed elsewhere.

VI. Impact Parameter Analysis

Information about analytic structure of the transform $T(q_{\parallel}, \vec{b})$ (of eq. (2.6)) in the impact parameter plane \vec{b} can be obtained from the behaviour of the amplitude A (as defined in eq. (3.3)). Such an analysis has been undertaken previously using canonical variables⁸⁾ different from ours with result showing some interesting regularities^{8,17)}. Using variables as defined in (2.4) we show a phenomenological analysis of differential cross section for pp scattering for fixed q_{\parallel} and varying q_{\perp} (i.e. t) in Fig. 7, for the values $q_{\parallel} = 0.48, 0.96, 1.31, 1.60, 2.54$ GeV. Unfortunately, unlike in ref. /8/, our curves $q_{\parallel} = \text{const}$ cross the experimentally measured area in s, t variables only in few points and our statistics is rather poor, weakening the conclusions drawn from this analysis. To improve this situation more measurements in the $90^{\circ} < \theta_{\text{cms}} < 180^{\circ}$ region would be necessary.

In spite of poor statistics two features of data seem apparent from Fig. 7.

1. At small values of q_{\parallel} one may get a fair parametrization of the data by a linear curve corresponding to $\frac{d\sigma}{dt} \sim \exp(-R_0 q_{\perp})$, whereas at large q_{\parallel} the data clearly curve up reflecting powerlike behaviour. The first case corresponds to pure GS, the second may be an indication of an extra component from parton picture¹⁷⁾ dominating at large q_{\perp} . From the point of view of analytic structure in the impact parameter plane the former corresponds to a pair of singularities at $b = \pm iR_0$, the latter to a singularity at $b = 0$.

2. The small q_{\perp} data if approximated by straight lines seem to have the slopes increasing with q_{\parallel} . In GS picture this would correspond to interaction radius growing with energy, the behaviour observed also in ISR region.

The analytic structure in the impact parameter plane may thus be quite complicated and we have not attempted to reproduce it by our profile parametrizations in section IV since they are completely regular and our model cannot be expected to work in this energy region (down to 1 GeV).

What comes out of the discussed phenomenological analysis is however believed to be of importance since the use of canonical variables should imply that the impact parameter structure reflects a real geometric property of physical particles. In particular, as the analysis in refs. /8/ and /17/ has shown, the existence of singularities at $b = \pm iR_0$ may mean that each particle could be ascribed a certain radius which characterizes it independently of whether it scatters elastically or is inclusively produced from any initial state. Whether this kind of universality holds also in the case of our variables remains to be checked by the analysis of the other reactions.

VII. Discussion

The assumption of adding a relativistic potential interaction to a geometrical scaling part has been tested in various ways. For the $\sigma_{tot}(pp)$ it turns out that the energy dependence connected with the potential term gives rise to GS corrections where the leading (and most important) terms of type $1/\sqrt{s}$ and $1/s$ describe the data quite well. A formal connection between a Regge approach (i.e. ρ , ω , and π exchanges) may be noted. Comparison with $\rho|_{t=0}$ data also shows the correct energy dependence.

The results favour slightly a $\ln^2 s$ type parametrization of asymptotic cross sections. The specific nature of the potential appears more clearly from $\frac{d\sigma}{dt}$, however as noted we do not predict a dip at $p_{lab} = 200$ GeV although we have one at higher energies. To understand the experimental dip new elements have to be introduced, possibly spin effects or a different form of the potential $V(r)$. The main features of $\bar{p}p$ scattering can also be understood within our framework, although some details still remain to be worked out. Extension of the approaches to other scattering processes like $\pi^\pm p$, $K^\pm p$ should be fairly straightforward.

Acknowledgement

Discussions with Drs. L. Łukaszuk, A. Bechler, F. Elvekjaer and F. Gutbrod are gratefully acknowledged. One of the authors (Z.J.R.) would like to express his gratitude to Professors H. Schopper, G. Weber and H. Joos for their hospitality at DESY.

Appendix

We use a covariant normalization

$$\langle q'_{\parallel}, \vec{q}'_{\perp} | q_{\parallel}, \vec{q}_{\perp} \rangle = (2\pi)^3 4 WW' \delta(q'_{\parallel} - q_{\parallel}) \delta(\vec{q}'_{\perp} - \vec{q}_{\perp}) \quad (\text{A.1})$$

so that

$$\langle q'_{\parallel}, \vec{b}' | q_{\parallel}, \vec{b} \rangle = (2\pi)^3 \delta(\vec{b} - \vec{b}') \delta(q'_{\parallel} - q_{\parallel}) \quad (\text{A.2})$$

The completeness of the IPS corresponding to the completeness of the plane wave states is expressed by

$$\frac{1}{(2\pi)^3} \int dq_{\parallel} d^2b |q_{\parallel}, \vec{b}\rangle \langle q_{\parallel}, \vec{b}| = 1 \quad (\text{A.3})$$

The matrix elements of the scattering matrix between plane wave states for the process $q_1 + q_2 \rightarrow p_1 + p_2$ can be written

$$\langle p_1, p_2 | T | q_1, q_2 \rangle = (2\pi)^4 \delta(p_1 + p_2 - q_1 - q_2) F(s, t) \quad (\text{A.4})$$

and going to the c.m. system we get

$$\langle p | T | q \rangle = \frac{W^2}{q\sqrt{s}} F(q_{\parallel}, \vec{q}_{\perp}) \delta(p_{\parallel} - q_{\parallel}) \delta(\vec{p}_{\perp} - \vec{q}_{\perp}) \quad (\text{A.5})$$

with the dependence of F now written in terms of q_{\parallel} and q_{\perp} using (2.4) and the factor in front is the appropriate phase space Jacobian with $q = (q_{\parallel}^2 + q_{\perp}^2)^{1/2}$. Also s is given by (2.4).

The impact parameter transform of T is defined by taking matrix elements between initial states $|i\rangle = |q_{\parallel}, \vec{b}_i\rangle$ and final states $|f\rangle = |p_{\parallel}, \vec{b}_f\rangle$ with $p_{\parallel} = q_{\parallel}$, i.e. $\langle f | T | i \rangle = T(q_{\parallel}, \vec{b}_i, \vec{b}_f) \delta(q_{\parallel} - p_{\parallel})$.

This leads to the relation

$$\begin{aligned}
 \langle p_{\parallel}, \vec{b}_f | T | q_{\parallel}, \vec{b}_i \rangle &= \frac{1}{(2\pi)^6} \int \frac{dp'_{\parallel} d^2 p'_{\perp}}{(2W')^2} \frac{dq'_{\parallel} d^2 q'_{\perp}}{(2W)^2} \\
 &\times \langle p_{\parallel}, \vec{b}_f | p'_{\parallel}, \vec{p}'_{\perp} \rangle \langle p' | T | q' \rangle \langle q'_{\parallel}, \vec{q}'_{\perp} | q_{\parallel}, \vec{b}_i \rangle \quad (A.6) \\
 &= \delta(p_{\parallel} - q_{\parallel}) \int \frac{d^2 q_{\perp}}{(2\pi)^4} e^{-i\vec{q}_{\perp} \cdot (\vec{b}_i + \vec{b}_f)} \frac{F(q_{\parallel}, \vec{q}_{\perp})}{4q\sqrt{s}}
 \end{aligned}$$

giving

$$T(q_{\parallel}, \vec{b}) = \int \frac{d^2 q_{\perp}}{(2\pi)^2} e^{-i\vec{q}_{\perp} \cdot \vec{b}} \frac{F(q_{\parallel}, \vec{q}_{\perp})}{4q\sqrt{s}} \quad (A.7)$$

where we have used the relations

$$\frac{1}{(2\pi)^3} \int \frac{dq'_{\parallel}}{(2W')^2} |q'_{\parallel}, \vec{q}'_{\perp}\rangle \langle q'_{\parallel}, \vec{q}'_{\perp}| = 1 \quad (A.8)$$

and

$$\langle q'_{\parallel}, \vec{b} | q_{\parallel}, \vec{q}_{\perp} \rangle = (2\pi)^2 2W \delta(q'_{\parallel} - q_{\parallel}) e^{i\vec{q}_{\perp} \cdot \vec{b}} \quad (A.9)$$

As one might expect the impact parameter transform depends only on the relative impact parameter $\vec{b} = \vec{b}_i + \vec{b}_f$ (we have a plus sign because the initial and final states have transverse planes which are connected by a coordinate inversion). In (A.7) $T(q_{\parallel}, \vec{b})$ is seen to be dimensionless since $F(q_{\parallel}, \vec{q}_{\perp})$ is the invariant Feynman amplitude and one may notice the factor $(q\sqrt{s})^{-1}$ with its specific dependence on the integration variable \vec{q}_{\perp} .

References

1. C. Bourrely et al., preprint ANL-HEP-PR-75-41
2. J. Dias de Deus, Nucl. Phys. B59, (1973) 231,
A.J. Buras and J. Dias de Deus, Nucl. Phys. B71 (1974) 481
3. Z. Koba, H.B. Nielsen and P. Olesen, Nucl. Phys. B40 (1971) 317
4. R.J.N. Phillips, Rutherford Lab. preprint 74-034,
W. Grein, R. Guigas and P. Kroll, Nucl. Phys. B89 (1975) 93,
W. Grein and P. Kroll, Phys. Lett. 58B (1975) 79,
V. Barger, J. Luthe and R.J.N. Phillips, Nucl. Phys. B88 (1975) 237
5. N.N. Khuri and T. Kinoshita, Phys. Rev. 137B (1965) 720
6. E.A. Bartnik, A.M. Din, J.M. Namysłowski and Z. Rek,
Göteborg Univ. preprint 75/25
7. N.P. Chang and K. Raman, Phys. Rev. 181 (1969) 2048,
N.P. Chang and K. Raman, *ibid.* 183 (1969) 1446,
N.P. Chang, Phys. Rev. 172 (1968) 1796,
H.I. Miettinen, IX Rencontre de Moriond (1974)
8. F. Elvekjaer and J.L. Petersen, Nucl. Phys. B94 (1975) 100,
F. Elvekjaer, CERN-TH 2067 (1975)
9. J. Dias de Deus, Nuovo Cim. 28A (1975) 114,
A. Martin, X Rencontre de Moriond (1975),
J. Fröyland, Phys. Lett. 58B (1975) 317,
J. Fröyland and H. Högaasen, Phys. Lett. 58B (1975) 319,
R. Torgerson and A.N. Kamal, Lett. Nuovo Cim. 13 (1975) 591
10. S. Weinberg, Phys. Rev. 150 (1966) 1313,
S.J. Chang and S.-K. Ma, Phys. Rev. 180 (1969) 1506,

11. J.M. Namysłowski, Lett. Nuovo Cim. 5 (1972) 991,
J.M. Namysłowski, Warsaw Univ. preprint 9/75
12. A.N. Diddens, Proc. XVII Int. Conf. on high energy physics,
London (1974),
V. Barger, ibid.
13. E. Bracci et al., CERN-HERA 73-1 (1973),
U. Amaldi et al., Phys. Lett. 44B (1973) 112,
S.R. Amendolia et al., Phys. Lett. 44B (1973) 119,
A.S. Carroll et al., Phys. Rev. Lett. 33 (1974) 928,
A.S. Carroll et al., Fermilab-Pub-75/51-EXP,
A.M. Wetherell, EPS Conference, Palermo 1975
14. K.J. Foley et al., Phys. Rev. Lett. 19 (1967) 857,
G.G. Beznogikh et al., Phys. Lett. 39B (1972) 411,
U. Amaldi et al., Phys. Lett. 43B (1973) 231,
N. Bartenev et al., Phys. Rev. Lett. 31 (1973) 1367,
C. Ankenbrandt et al., Fermilab Conf. 75/61-EXP
15. R.M. Edelstein et al., Phys. Rev. D5 (1972) 1073,
A. Böhm et al., Phys. Lett. 49B (1974) 491,
N. Kwak et al., Phys Lett. 58B (1975) 233,
C.W. Akerlof et al., Phys. Rev. Lett. 35 (1975) 1406,
C.W. Akerlof et al., Phys. Lett. 59B (1975) 197
16. C.W. Akerlof et al., Univ. of Michigan preprint UM HE 75-21
17. F. Elvekjaer, Nucl. Phys. B101 (1975) 112,
F. Elvekjaer and F. Steiner, DESY 75/49 (1975)

Figure Captions

Fig. 1. The total, inelastic and elastic pp cross section. The full lines correspond to the solution (4.8b), the dashed lines to the Barger fit ¹²⁾ (see section 4). Of each pair of similarly drawn curves for σ_{tot} the lower one corresponds to GS contribution only. The data are taken from ref. 13.

Fig. 2. $\rho = \frac{\text{Re } A}{\text{Im } A} \Big|_{t=0}$ for pp scattering. The data are from ref. 14.

Fig. 3. $\left(\frac{d\sigma}{dt}\right)_{pp}$ for

a) $p_{\text{lab}} = 21.1$ and 1496 GeV,

b) $p_{\text{lab}} = 29.7, 69, 100, 200, 281$ and 2048 GeV.

Data are from refs. 13 and 15.

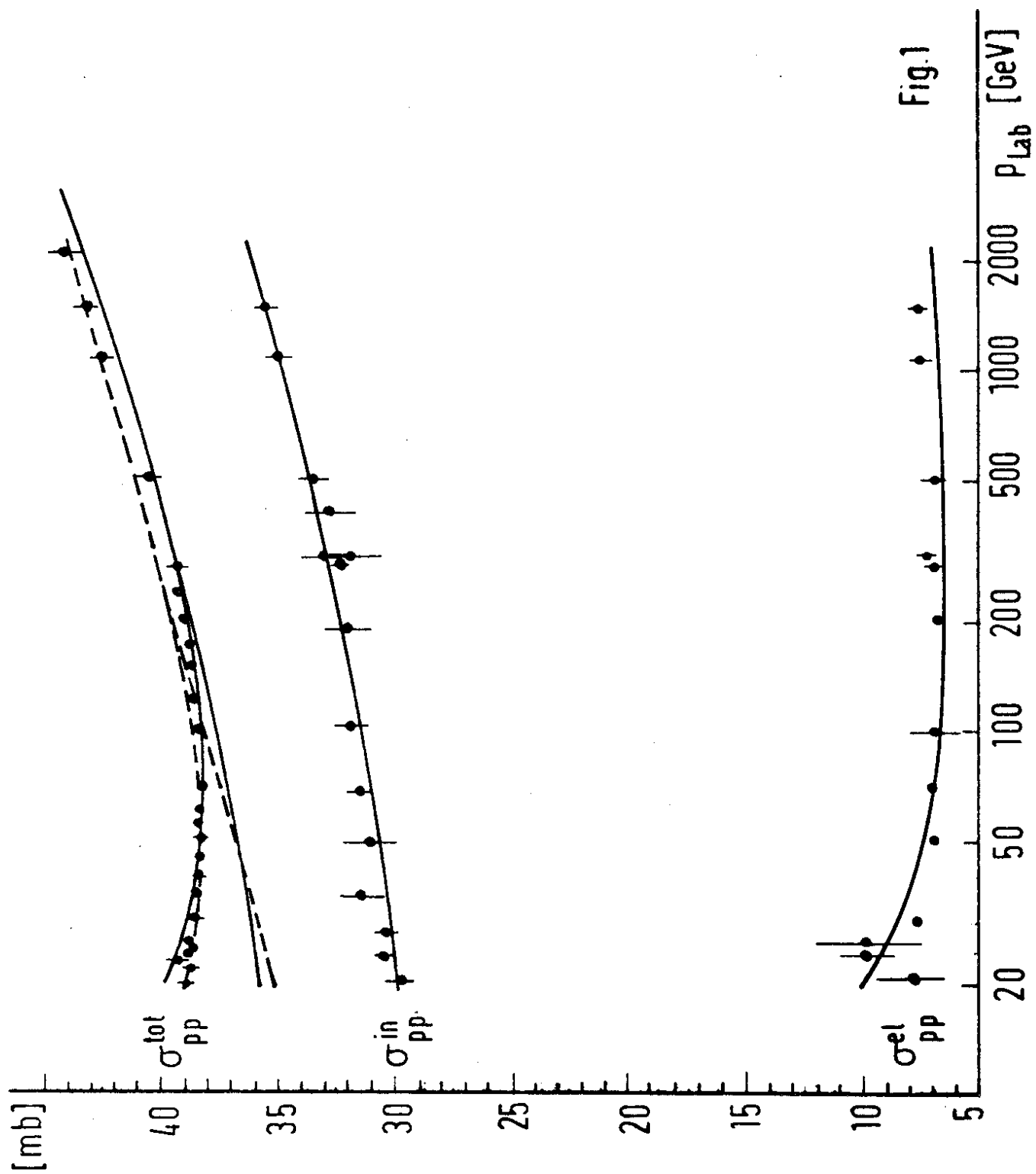
Fig. 4. Total, inelastic and elastic $\bar{p}p$ cross section. Data are from ref. 13.

Fig. 5. $\rho = \frac{\text{Re } A}{\text{Im } A} \Big|_{t=0}$ for $\bar{p}p$ scattering. Data are from ref. 14.

Fig. 6. $\left(\frac{d\sigma}{dt}\right)_{\bar{p}p}$ for $p_{\text{lab}} = 50, 100, 200$ GeV. Data are from ref. 16.

Fig. 7. $\left(\frac{d\sigma}{dt}\right)_{pp}$ as a function of q_{\perp} for the fixed values of

$q_{\parallel} = 0.48, 0.96, 1.31, 1.60$ and 2.54 GeV. The straight lines are drawn only "to guide the eye".



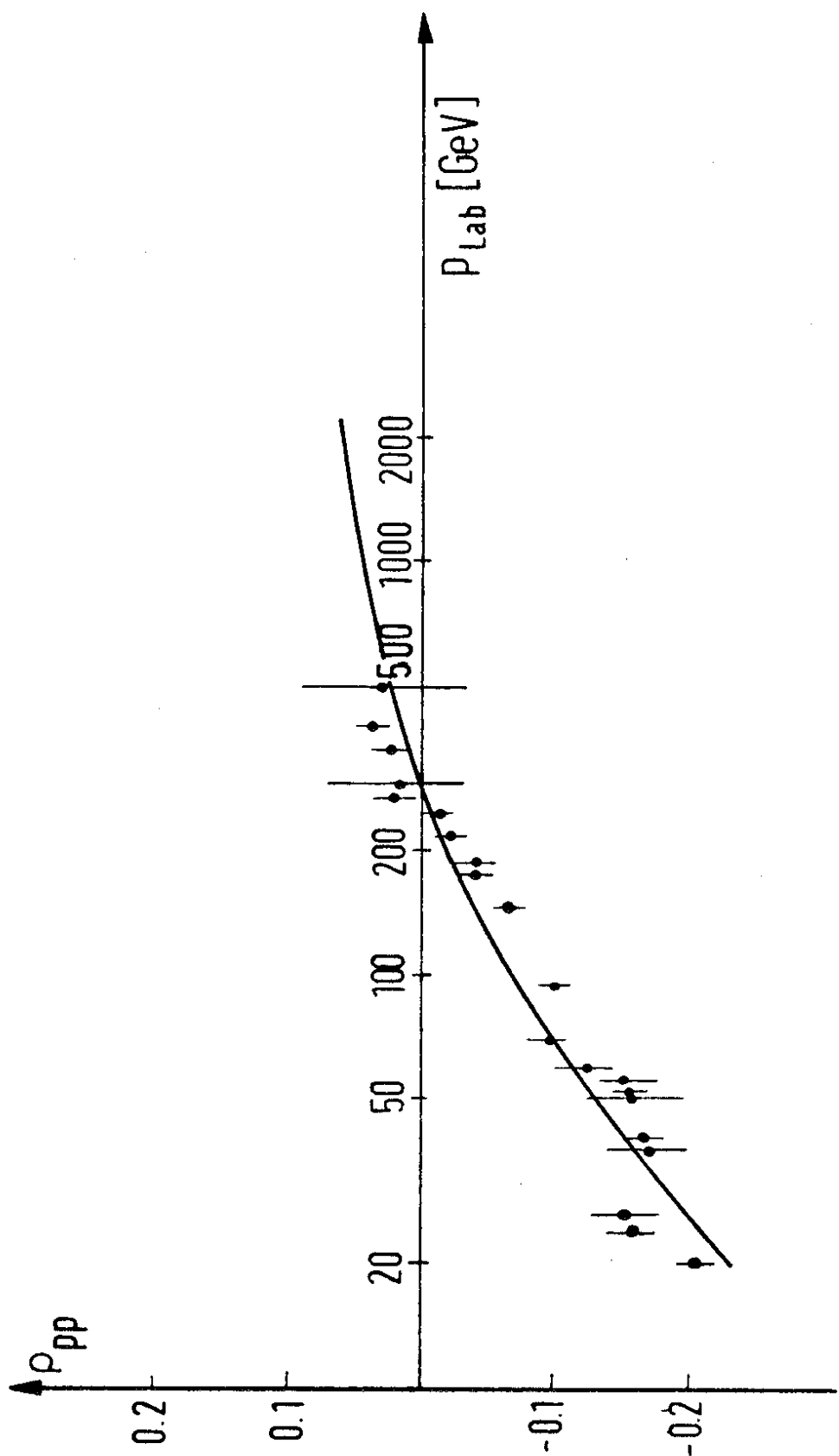
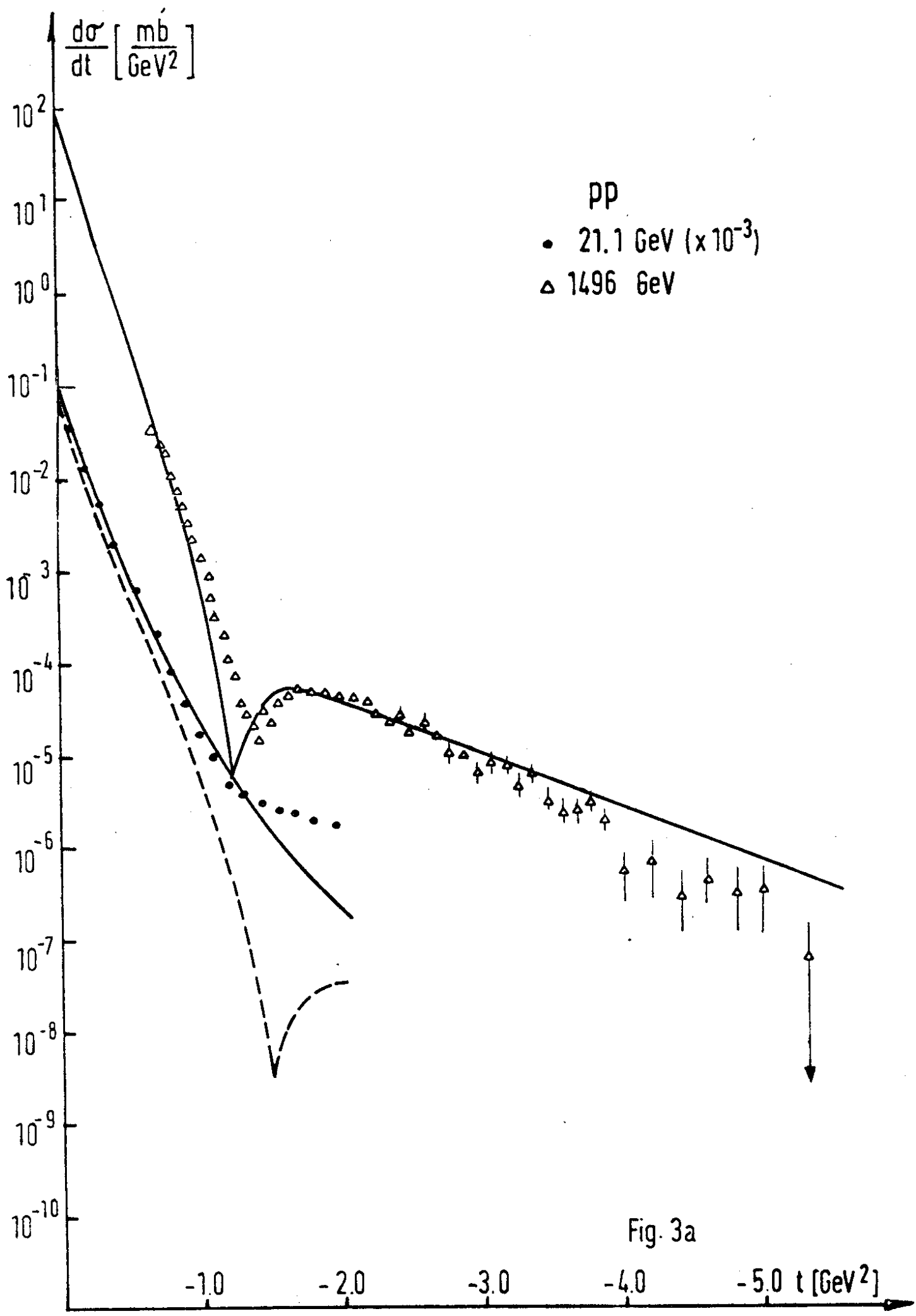


Fig.2



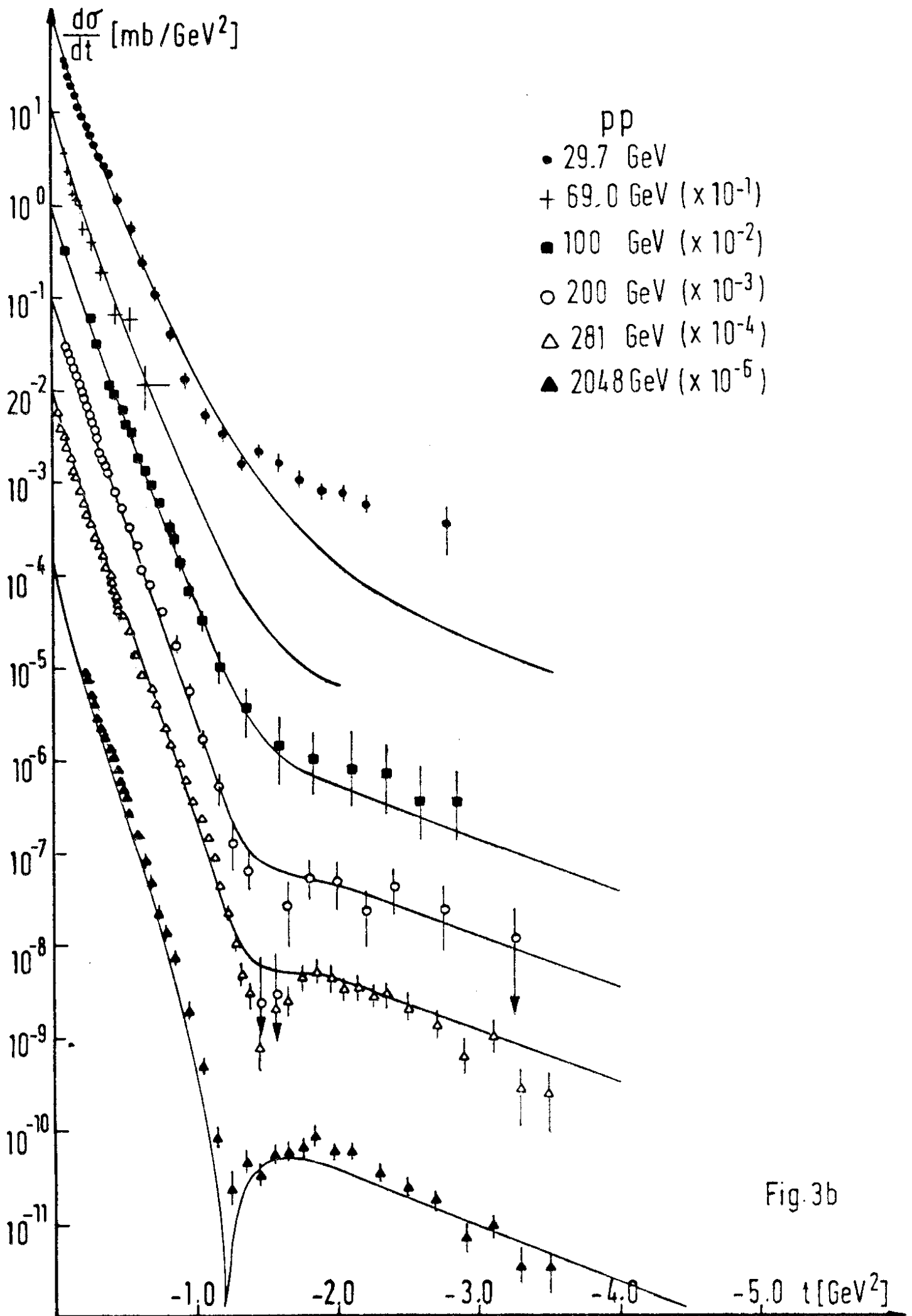


Fig. 3b

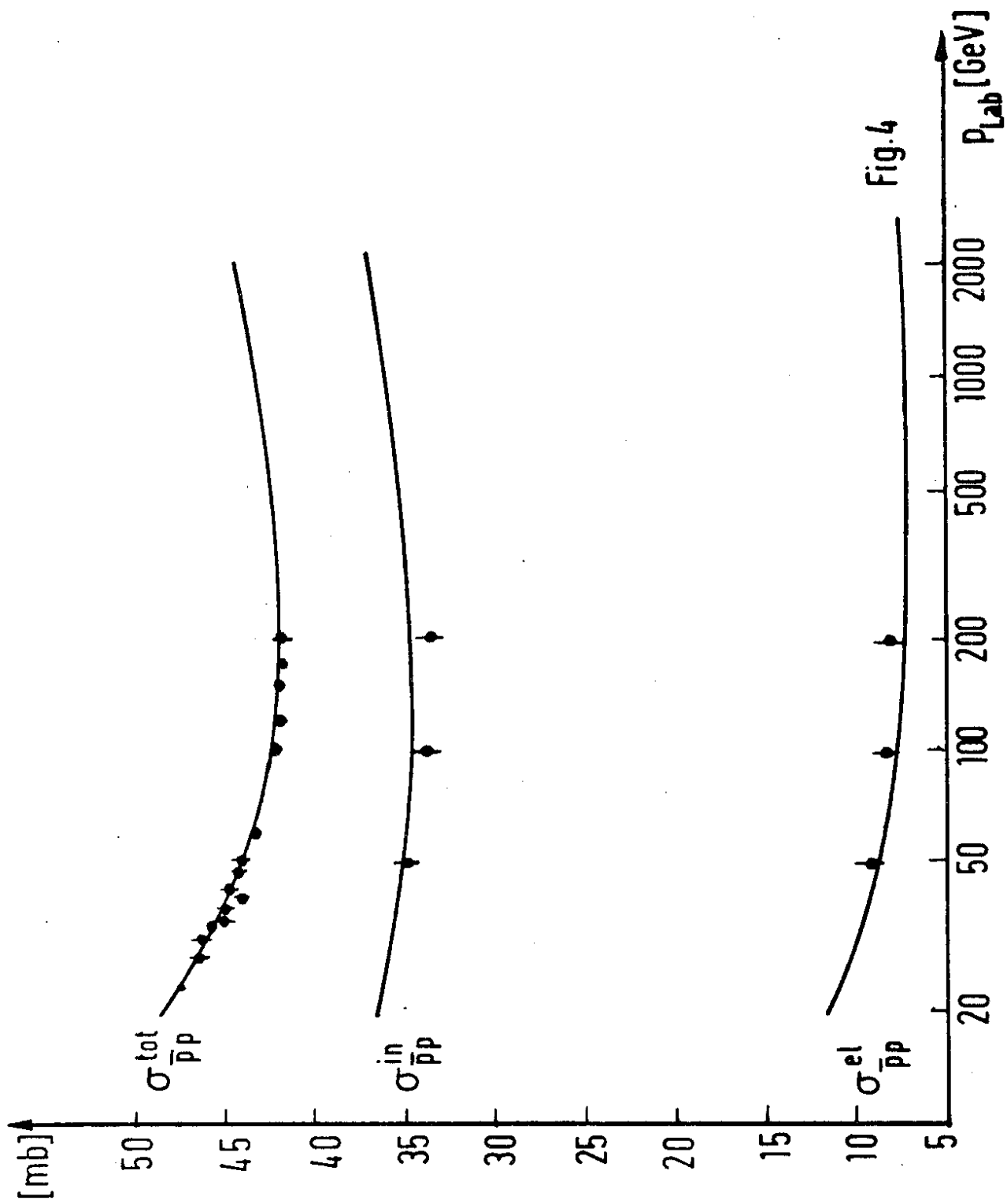


Fig.4

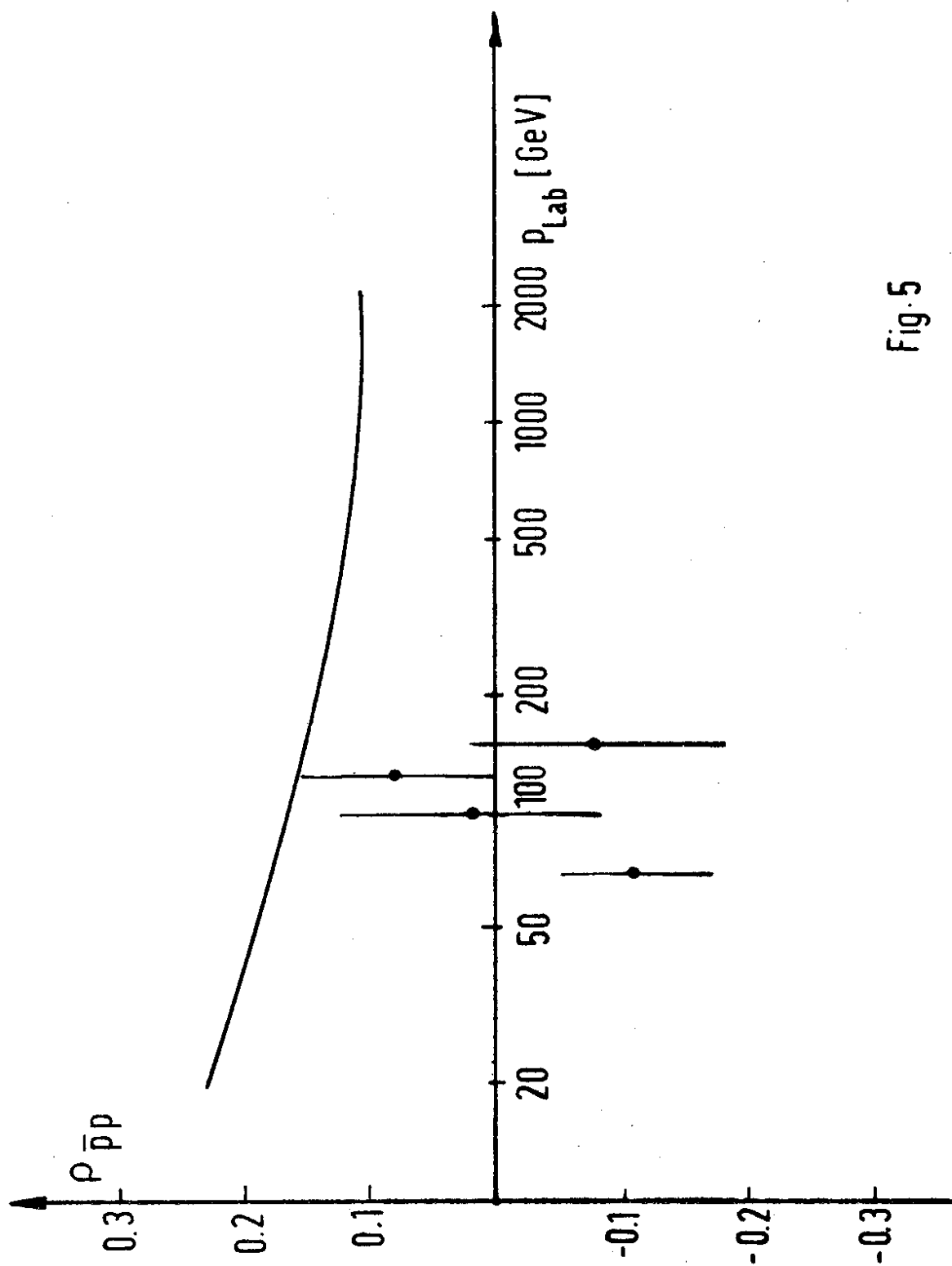


Fig. 5

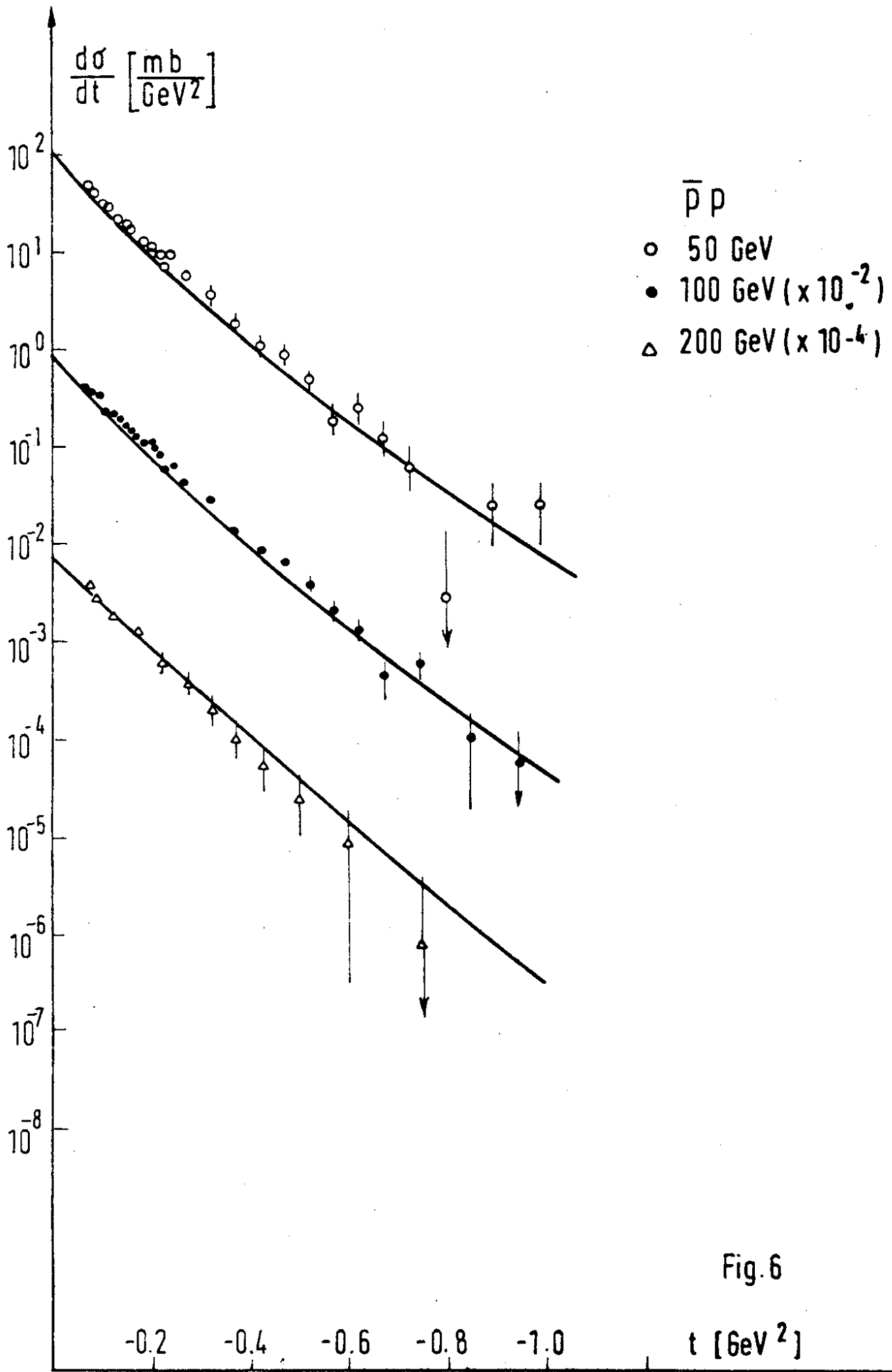


Fig. 6

